SSRG International Journal of Recent Engineering Science
ISSN: 2349–7157 / https://doi.org/10.14445/23497157/IJRES-V11I5P119

Volume 11 Issue 5, 193-205, Sep-Oct 2024

Original Article

Application of a Hybrid Cell-in-Series Model for Simulating Phosphorus Transport in Ureje River, Southwestern Nigeria

Ayeni. A.T[1], Ayeni. O.O[2], Olowe. K.O[3]

[1,3]*Department of Civil Engineering, Afe Babalola University Ado Ekiti (ABUAD).*
[2]*Department of Civil Engineering. The Federal Polytechnic, Ado Ekiti.*

[1]*Corresponding Author : Ayeni_oo@fedpolyado.edu.ng*

Received: 26 August 2024 Revised: 30 September 2024 Accepted: 16 October 2024 Published: 30 October 2024

Abstract *- The Hybrid Cell In-Series (HCIS) model was employed to assess nutrient influx into River Ureje as a surface water quality monitoring tool. Other models struggled to predict solute transport due to difficulties in estimating the longitudinal dispersion coefficient and theoretical limitations. This led to the adoption of the HCIS model for predicting phosphorus movement in River Ureje. A mass balance approach was used to create a basic hybrid model comprising a plug flow cell and two fully mixed cells, all connected in series. This model was designed to simulate the first-order kinetic reaction of phosphorus, as well as advection and dispersion processes, to track nutrient movement from a single point source. Analytical solutions for the model and nutrient kinetics were derived using Laplace transformation and then implemented through the C-Sharp programming language. A user-friendly software was developed to forecast temporal and spatial fluctuations in nutrient concentration. The model's ability to predict phosphorus concentration was tested using both hypothetical data and field data collected from Ureje River from September 2023 to March 2024. Analytical solutions proved effective in estimating nutrient and solute movement within the river, verifying the model's accuracy.*

Keywords *- River Ureje, Hybrid Cell in-Series Model, Phosphorus, Advection-Dispersion Equation model.*

1. Introduction

Climatic changes and human activities contribute to increased nutrient pollution in rivers and streams, leading to deteriorating water quality and threatening ecosystems [1][2]. The Ureje River in Ado Ekiti faces similar challenges, which concern Afe Babalola University (ABUAD) as the institution's growing population and infrastructure require a reliable water supply. Currently, the university's groundwater sources are insufficient, necessitating research into alternative water sources, such as surface water, within the university's boundaries. This research involves continuous monitoring of nutrient pollutants, which is essential for designing a reservoir and water treatment facility. While nutrients are necessary for aquatic life, excessive amounts can cause problems like eutrophication, which negatively impacts biodiversity, drinking water quality, and recreational water use [3], [4]. Over-enrichment of nutrients can also lead to harmful algal blooms that produce toxins, contaminate drinking water, and diminish the aesthetic quality of rivers [5], [6] classified nutrient pollutants into conservative pollutants, which do not degrade but may change in form, and non-conservative pollutants, which degrade over time. Existing water quality models have struggled to predict solute transport, particularly due to challenges in estimating the longitudinal dispersion coefficient and other theoretical limitations [5]. These shortcomings create inconsistencies in the simulation of pollutant transport and hinder effective water quality management. Many traditional models, like the Streeter and Phelps model, have been found inadequate for modern applications involving complex nutrient dynamics in rivers [7]. In response, Ghosh developed the Hybrid Cell in Series (HCIS) model in 2004, which improves on earlier models [8], [9]. This research adopts the Hybrid Cell in-Series (HCIS) model, a more robust approach for predicting phosphorus movement in rivers. The HCIS model overcomes the limitations of previous models by combining a mass balance approach with a hybrid design, which consists of a plug flow cell and two fully mixed cells arranged in series. This model accurately simulates first-order kinetic reactions of phosphorus along with advection and dispersion processes. Furthermore, the use of analytical solutions derived through Laplace transformation and implemented via the C-Sharp programming language enhances the model's predictive accuracy to simulate phosphorus transport in the Ureje River, which runs through Afe Babalola University. The Ureje River flows through the city of Ado Ekiti, including the campus of Afe Babalola University, before ultimately draining into the Ogbesse River near the Ado/Afao Road (Figure 1).

Fig. 1 Map of Ureje River as it flows through ABUAD University Property (Copied from Google Earth Map)

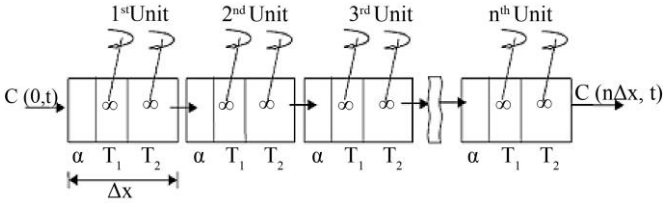

Fig. 2 A conceptualized hybrid unit of Hybrid Cells in a Series Model [13]

Excessive phosphorus in the Ureje River has significant environmental and ecological consequences [10]. Phosphorus is a key contributor to eutrophication, where nutrient over-enrichment stimulates excessive algae growth [11]. This leads to oxygen depletion, creating dead zones that disrupt aquatic life [4]. Harmful algal blooms (HABs), often triggered by high phosphorus levels, produce toxins that contaminate drinking water, harm aquatic organisms, and affect recreational use [2]. Phosphorus pollution degrades water quality, making it unsuitable for consumption and irrigation while complicating water treatment processes [12]. This pollution can result in a decline in biodiversity as aquatic species struggle to survive in low-oxygen conditions. For Afe Babalola University (ABUAD), which depends on the river for water resources, excessive phosphorus increases the cost and complexity of water management. Addressing phosphorus pollution is vital to preserve the river's ecosystem and maintain water quality for both the university and surrounding communities.

2. Theoretical Analysis

2.1. Development of a Conceptual Hybrid Cell-in-Series Model with Integrated Phosphorus Nutrient Equation"

The Hybrid Cell-in-Series (HCIS) model developed by Ghosh in 2004 was to address the limitations of the conventional Cell-in-Series (CIS) and Advection Dispersion Zone (ADZ) models, specifically in their ability to simulate pollution transport pathways effectively [6], [13], [14] As illustrated in Figure 2, the HCIS model consists of a sequence of hybrid units designed better to replicate the behavior of pollutants in water bodies.

Each hybrid unit comprises a plug flow cell, which simulates uniform pollutant movement, and two fully mixed cells that represent areas of complete mixing. These units are arranged in series to provide a more accurate representation of the pollutant transport dynamics.

The notion of water quality mass balancing equation created for the phosphorus concentration in the component of the HCIS model under steady-state conditions underpins the derivative of the model to be coupled with the first-order kinetic reaction of the phosphorus reaction. The first-order kinetic equation of phosphorus concentration is represented by the differential equation below (Vesientutkimuslaitoksen, 1982)

$$\frac{dC_p}{dt} + \frac{\mu dC_p}{dx} = (-\mu + \rho)\alpha_1 A + \alpha_p\, C_p(\mathrm{x,t}) \qquad (1)$$

In this model, x represents the distance along the river (m), t is the time (sec), and Cp is the phosphorus concentration (mg/L) Figure 3. The algae growth rate coefficient is (day−1), z is the mean stream depth (m), and fp is the phosphorus fraction of algal biomass. Ag is the algal biomass concentration (mg/L) and is the algae respiration rate coefficient (day−1), which increases phosphorus in the water column.

The first term of the equation models phosphorus uptake by phytoplankton and its conversion to orthophosphate via respiration. The second term describes phosphorus input from algae respiration and nutrient uptake by algae. The third term represents phosphorus release from benthic processes. The rate of change in algal biomass is governed by the following differential equation [8].

$$\frac{\partial A_g(t)}{\partial t} = (\mu - \rho)A_g(t) \qquad (2)$$

The model development focuses on a river reach composed of hybrid components, each including a plug flow cell and two well-mixed cells connected in series with different residence times (T1, T2, T3). At time t = 0, the phosphorus concentration ranges from zero to CR. The plume in the plug flow cell is replaced over time T1, calculated as the cell volume divided by the flow rate. As phosphorus moves downstream, a fraction is lost due to bacterial absorption and algae conversion.

The first well-mixed cell has a residence time of T2, and after mixing, the fluid enters the second well-mixed cell (T3). Phosphorus transport follows first-order reactions in plug flow with minimal dispersion, while advection-dispersion occurs in the well-mixed cells. The system is modeled as a series of hybrid cells to estimate phosphorus levels in the river.

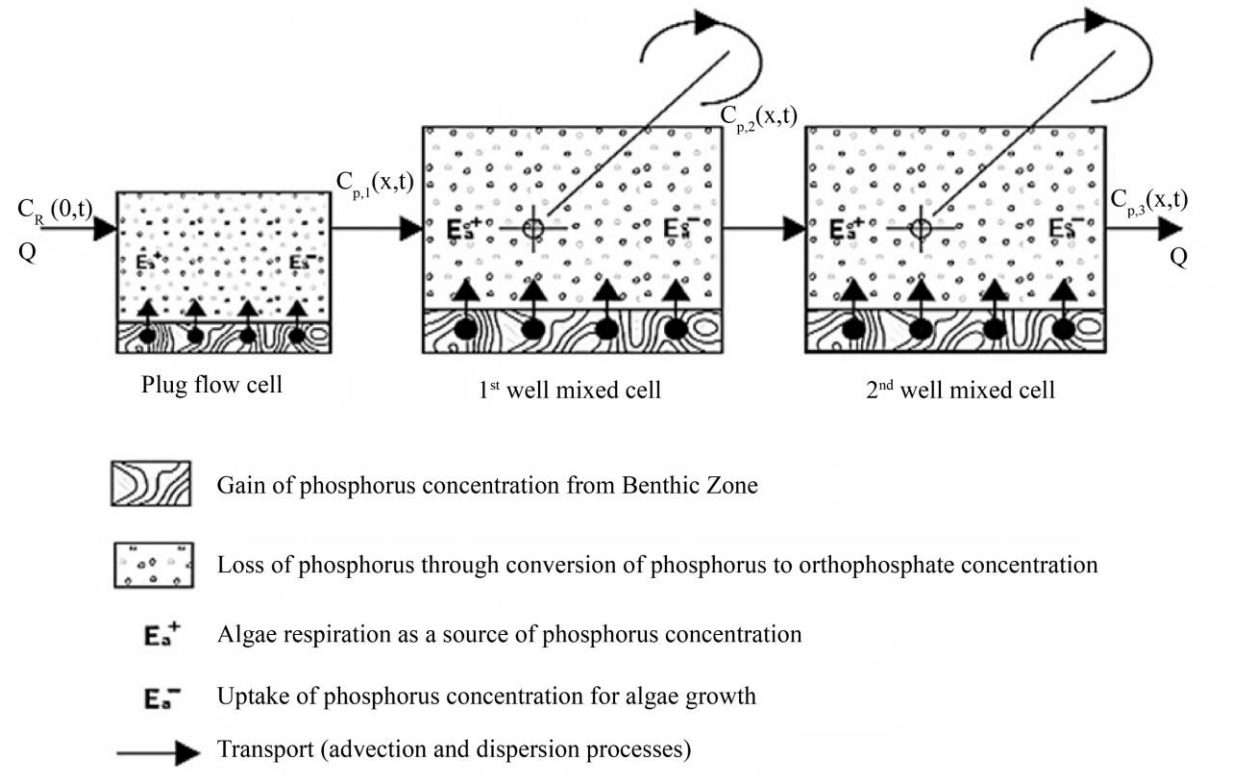

Fig. 3 The Process of Phosphorus Pollutant Concentration through a Hybrid Unit

2.2. Phosphorus Dynamics in a Plug Flow Cell

Figure 4 illustrates a control volume (V) where a non-conservative phosphorus pollutant is transported downstream within a plug flow cell. In this setup, the phosphorus solute moves without altering its concentration, represented as Cp at any location (x, t). Phosphorus undergoes eutrophication, transforming into orthophosphate and being partially absorbed by algae, which reduces its concentration. Algal respiration and benthic phosphorus release also add to the phosphorus levels in the water. The remaining pollutant then flows into the subsequent control volume. Algal biomass further depletes dissolved oxygen, impacting overall water quality. Under steady-state conditions, a mass balance for the phosphorus pollutant is established using a second-order partial differential equation. The final concentration of phosphorus is measured in the effluent of the plug flow cell, offering essential insights into pollutant dynamics within the water system.

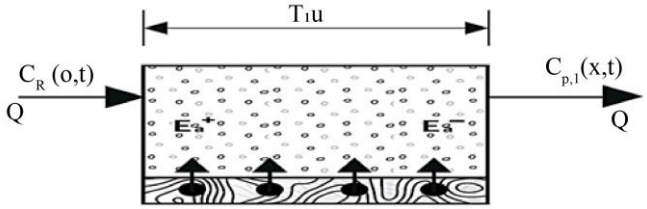

Fig. 4 The process of concentration of Phosphorus pollutant through a plug flow cell

Equation (1) is solved with the initial and boundary conditions such as $C_p(x,0) = 0$ for $x > 0$; $C_a(0, t) = C_R$ for $t \geq 0$; $C_p(T_1u, t) = 0$ for $0 < t < T_1$.

The algae biomass equation in Eq. (3) has a solution shown below.

$$A_g(t) = A_o\, e^{(\mu-\rho)\tau} \tag{3}$$

The above equation can be modified to express $A_g(x, t)$ for a constant initial (A_0) at a distance of x to a control volume within the plug flow cell.

$$A_g(t) = A_o\, e^{(\mu-\rho)(t-\frac{x}{u})} \tag{4}$$

Taking Laplace transform of each term in Equation (1) and rearranging

$$\frac{dC_p}{dx} = \frac{(s+\propto_p)}{u} C_p + (\rho-\mu)\alpha_1 A l^{-(\mu-\rho)\frac{x}{\mu}} + \frac{\gamma_p}{UZ} \tag{5}$$

Solving Equation (5) with differential equation and taking the inverse Laplace Transformation at the end of plug flow.

$$C_{P1}(x,t) = \left[\left[C_R U(t-T_1)\ell^{-\alpha p T1}\right] + \left[(\rho-\mu)\alpha_1 A_\circ \ell^{-(\mu-\rho)T_1}\{\varphi\}\right] - \left[(\rho-\mu)\alpha_1 A_\circ U(t-T_1)\ell^{-\alpha p T1}\{\phi\}\right] - \left[\frac{\gamma_p}{Z} U(t-T_1)\ell^{-\alpha p T1}\{\psi\}\right]\right]$$

Where

$$\emptyset = \left(\frac{1}{\alpha\rho}(\ell^{-(\rho-\mu)t} - \ell^{-(\propto\mu+\rho-\mu)t}\right) + (\frac{\gamma_p}{z}\{\frac{1}{\alpha p}(\ell^{-\alpha pt})\}$$

$$\Psi = \{\left(\frac{1}{\alpha\rho}(\ell^{-(\rho-\mu)t-T1})\right\} - \{\ell^{-(\propto\mu+\rho-\mu)t-T1}\right)$$

$$\phi = \{\left(\frac{1}{\alpha\rho}\ell^{-\alpha p(t-T1)}\right) \quad (6)$$

Pollutant at the end of Plug Flow

The concentration of phosphorus pollutant at the end of the plug flow cell is obtained as follows by solving Equation (6) using the inverse Laplace transform and is valid for t T1.

$$C_{a,1}(T_1u,t) = C_R U(t-T_1)e^{-k_aT_1} - \left[\frac{\rho\alpha A_o - F\alpha\mu A_o}{ka}U(t-T_1)e^{-k_aT_1} - 1\right]\left(e^{-(\rho-\mu)(t-T_1)}\right) - \frac{\delta_3 e^{-k_at}}{d.k_a}[(U(t-T_1)-1)] \quad (7)$$

Where U (t-T_1) is the step function.

2.3. Phosphorus Concentration Derivation in the First Fully Mixed Cell

Pollutants move a distance (T1u) from the plug flow cell into the first well-mixed cell, as shown in Figure 5. The filling time (T2) for this first well-mixed cell is determined by dividing the cell's volume (V2) by the flow rate (Q). In this cell, phosphorus pollutants start to break down, with part of the phosphorus concentration being reduced as it converts to orthophosphate through nitrification and is utilized by algae. Additionally, algal respiration and phosphorus release from benthic sediments further contribute to the total phosphorus concentration in the water. The phosphorus concentration in the first well-mixed cell is then calculated based on mass balance.

$$C_{p1}\,Q\Delta t - C_{p2}Q\Delta t + (\rho-\mu)\alpha_1 A v_2 Q\Delta t + \frac{\gamma_p V_{2\Delta t}}{Z} - \alpha\rho C_{p2}V_2\Delta t = V_2\Delta C_{p2} \quad (8)$$

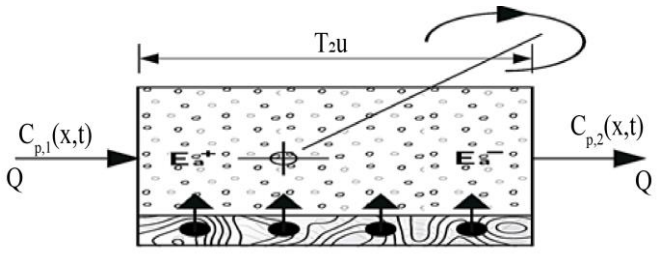

Fig. 5 The process of concentration of phosphorus pollutants through the first well-mixed cell

The first term on the left side represents the mass exiting the plug flow cell. The second term accounts for the mass leaving the well-mixed cell, while the third term describes the conversion of phosphorus into orthophosphate via nitrification. The fourth term represents phosphorus input due to algal respiration and uptake by algae. The fifth term indicates orthophosphate release from the benthic environment. The right side of the equation captures the change in mass within the cell. Equation (8) is then reformulated in differential form and solved, yielding the phosphorus concentration at the end of the first well-mixed cell in Equations (9) and (10).

$$\frac{dC_{P2}}{dt} + C_{P2}\left(\frac{1+T_2\alpha_p}{T_2}\right) = \frac{C_{P_1}}{T_2} + (\rho-\mu)\alpha_1 A + \frac{Y_p}{Z} \quad (9)$$

Solving this equation using a differential equation and the following solution was obtained at the end of the first well mixed cell.

$$C_{P2} = \begin{bmatrix} \left[\frac{C_R U(t-T_1)\ell^{-\alpha pT1}}{(1+\alpha pT_2)}\right] + \left[(\rho-\mu)\alpha_1 A_\circ \ell^{-(\mu-\rho)T_1}\frac{1}{\alpha p}\{\beta\}\right] \\ + \left[\frac{Y_P}{Z}\{\chi\}\right] - [(\rho-\mu)\alpha_1 A_\circ U(t-T_1)\ell^{-\alpha pT1}\{\delta\}] - \left[\frac{Y_P}{Z}U(t-T_1)\ell^{-\alpha pT1}\ell^{(t-T_1)\alpha p}\right] \\ + \left[\frac{(\rho-\mu)\alpha_1 A_\circ T_2}{(1+\alpha pT_2)}\right] + \left[\frac{Y_P T_2}{Z(1+\alpha pT_2)}\right] - \left[\frac{C_R U(t-T_1)\ell^{-\alpha pT_1}\ell^{\left(\frac{1+\alpha pT_2}{T_2}\right)(T_1-t)}}{(1+\alpha pT_2)}\right] \\ - \left[(\rho-\mu)\alpha_1 A_\circ \ell^{-(\mu-\rho)T_1}\frac{1}{\alpha p}\{\gamma\}\right] - \left[\frac{Y_P}{Z}\{\pi\}\right] + [(\rho-\mu)\alpha_1 A_\circ U(t-T_1)\ell^{-\alpha pT1}\{\varepsilon\}] \\ + \left[\frac{Y_P}{Z}U(t-T_1)\ell^{\left(\frac{1}{T_2}\right)(T_1-t)}\ell^{\alpha p}\right] - \left[\frac{(\rho-\mu)\alpha_1 A_\circ T_2\ell^{\left(\frac{1+\alpha pT_2}{T_2}\right)(T_1-t)}}{(1+\alpha pT_2)}\right] - \left[\frac{Y_P T_2\ell^{\left(\frac{1+\alpha pT_2}{T_2}\right)(T_1-t)}}{Z(1+\alpha pT_2)}\right] \end{bmatrix} \quad (10)$$

Whereby

$$\beta = \left[\frac{\ell^{-\frac{(T_2\rho-T_2\mu)t}{T_2}}}{(1+\alpha pT_2-T_2\rho+T_2\mu)} - \frac{\ell^{\frac{(\rho+\mu)}{T_2}}\ell^{-(\alpha p)t}}{(1-T_2\rho+T_2\mu)}\right]$$

$$\chi = \left[\frac{1}{\alpha p}\ell^{-(\alpha p)t}\right]$$

$$\delta = \left[\left(\frac{\frac{1}{\alpha p}\ell^{\frac{(T_2\rho-T_2\mu)t}{T_2}}\ell^{-(\rho-\mu)T_1}}{(1+\alpha pT_2-T_2\rho-T_2\mu)}\right) - \left(\frac{\ell^{-(\rho+\mu)t}\cdot\ell^{-(\alpha p)t}}{(1-T_2\rho+T_2\mu)}\ell^{-(\alpha p+\rho-\mu)T_1}\right)\right]$$

$$\gamma = \left[\frac{\ell^{\left(\frac{1+\alpha pT_2}{T_2}\right)(T_1-t)}\ell^{-(\rho-\mu)T_1}}{(1+\alpha pT_2-T_2\rho+T_2\mu)} - \frac{\ell^{\frac{(1-T_2\rho+T_2\mu)T_1}{T_2}}\ell^{-\left(\frac{1+\alpha pT_2}{T_2}\right)t}}{(1-T_2\rho+T_2\mu)}\right]$$

$$\pi = \left[\frac{1}{\alpha p}\ell^{\left(\frac{1}{T_2}\right)T_1}\ell^{-\left(\frac{1+\alpha pT_2}{T_2}\right)t}\right] \quad (11)$$

Equation (11) is the concentration of Phosphorus at the end of the first mixing cell.

2.4. Phosphorus Derivative in the Second Mixed Cell

The second mixed cell, as depicted in Figure 6, is thought to have a filling time of (T3). The inflow to the second well-mixed cell is equal to the outflow from the first well-mixed cell.

This cell is also where the phosphate pollutant decays and the phosphate concentration is added. The following is the mass balance in the second mixed cell.

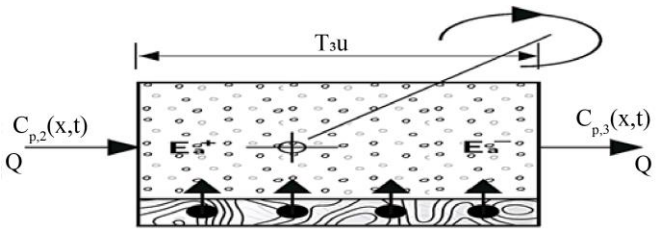

Fig. 6 The process of concentration of phosphate pollutant through the second well-mixed cell

The mass entering the cell is the first term on the left, the mass leaving the cell is the second, and the mass due to algal death and respiration is the third term. The mass attributable to benthic phosphate release in the water column is the last phrase on the left side. To find the step response function for phosphorus concentration at the end of the first hybrid unit, write Equation (11) in first order differential form, as given in Equation (12), and solve it.

$$\frac{dC_{p2}}{dt} + C_{p2}\left(\frac{1+T_2\propto\rho}{T_2}\right) = \frac{C_{p1}}{T_2} + (\rho-\mu)\alpha_1 A + \frac{\gamma_p}{z} \dots\dots (12)$$

Equation (11) was substituted to Equation (12) and solved with the integration method to determine the step response function for phosphate concentration at the end of the first hybrid unit.

Where

$$I = \left(\frac{T_2\ell^{\left(\frac{1+\alpha pT_2}{T_2}\right)T_1}\ell^{-\left(\frac{1+\alpha pT_2}{T_2}\right)t}\ell^{(\rho-\mu)T_1}T_2\ell^{\left(\frac{1+\alpha pT_2}{T_2}\right)T_1}\ell^{-\left(\frac{1+\alpha pT_2}{T_2}\right)T_1}\ell^{\left(\frac{1+\alpha pT_3}{T_3}\right)(T_1-t)}\ell^{(\rho-\mu)T_1}}{(1+T_2\alpha p)(1+T_3\alpha p)(1+T_2\alpha p-T_2\rho+T_2\mu)}\right) - \left(\frac{T_2\ell^{\left(\frac{1-T_2\rho+T_2\mu}{T_2}\right)T_1}\ell^{-\left(\frac{1+\alpha pT_2}{T_2}\right)t}\ell^{-\left(\frac{1+\alpha pT_2}{T_2}\right)T_1}\ell^{\left(\frac{1+\alpha pT_3}{T_3}\right)(T_1-t)}}{(1-T_2\rho+T_2\mu)(1+\alpha pT_2)(1+\alpha pT_3)}\right)$$

$$J = \left(\ell^{-\left(\frac{1+\alpha pT_2}{T_2}\right)t} - \ell^{-\left(\frac{1+\alpha pT_2}{T_2}\right)T_1}\ell^{\left(\frac{1+\alpha pT_3}{T_3}\right)(T_1-t)}\right)$$

$$K = \left(\frac{T_2\ell^{\left(\frac{1+\alpha pT_2}{T_2}\right)T_1}}{\alpha p(1+T_2\alpha p-T_2\rho-T_2\mu)(1+T_2\alpha p)(1+T_3\alpha p)}\left\{\ell^{-\left(\frac{1+\alpha pT_2}{T_2}\right)t} - \ell^{-\left(\frac{1+\alpha pT_2}{T_2}\right)T_1}\ell^{\left(\frac{1+\alpha pT_3}{T_3}\right)(T_1-t)}\right\}\right)\dots$$

$$L = \left(\ell^{-\left(\frac{1+\alpha pT_2}{T_2}\right)t} - \ell^{-\left(\frac{1+\alpha pT_2}{T_2}\right)T_1}\ell^{\left(\frac{1+\alpha pT_3}{T_3}\right)(T_1-t)}\right)..$$

$$M = \left(\ell^{-\left(\frac{1}{T_2}\right)t}\ell^{\alpha p} - \ell^{-\left(\frac{1}{T_2}\right)T_1}\ell^{\alpha p}\ell^{\left(\frac{1+\alpha pT_3}{T_3}\right)(T_1-t)}\right)\dots\dots\dots$$

$$N = \left(\ell^{-\left(\frac{1+\alpha pT_2}{T_2}\right)t} - \ell^{-\left(\frac{1+\alpha pT_2}{T_2}\right)T_1}\ell^{\left(\frac{1+\alpha pT_3}{T_3}\right)(T_1-t)}\right)$$

$$O = \left(\ell^{-\left(\frac{1+\alpha pT_2}{T_2}\right)t} - \ell^{-\left(\frac{1+\alpha pT_2}{T_2}\right)T_1}\ell^{\left(\frac{1+\alpha pT_3}{T_3}\right)(T_1-t)}\right)$$

$$P = \left(1 - \ell^{\left(\frac{1+\alpha pT_3}{T_3}\right)(T_1-t)}\right)$$

$$Q = \left(1 + \ell^{\left(\frac{1+\alpha pT_3}{T_3}\right)(T_1-t)}\right) \quad (13)$$

Equation (13) is used to forecast the fate of phosphorus pollutants that are transported due to phosphorus oxidation to nitrite, the algae process, and the benthic release of orthophosphate nitrogen.

3. Materials and Methods

3.1. Materials

River Ureje served as the study site for monitoring nutrient influx, mainly phosphorus concentrations, as part of the surface water quality analysis. Field data, including phosphorus measurements and other river morphological information, were collected from the river between September 2023 and March 2024. Additionally, hypothetical data were generated to evaluate the model's predictive capabilities in controlled environments. Analytical solutions were developed using the C-Sharp programming language to create user-friendly software for simulating and predicting nutrient concentrations. The Laplace transformation was applied to derive these solutions, enabling the modeling of phosphorus transport and kinetics.

The Hybrid Cell-in-Series (HCIS) model was composed of three main components:

- Plug Flow Cell: Simulates the advection and dispersion of phosphorus.
- Two Fully Mixed Cells: Connected in series to model the kinetic reactions of phosphorus in the river.
- Nutrient Kinetics Analysis: Utilized a first-order kinetic reaction framework to represent phosphorus behavior within the system.

3.2. Methods

The Hybrid Cell-in-Series (HCIS) model was developed using a mass balance approach to simulate phosphorus transport and reactions in River Ureje. This model comprises a plug flow cell followed by two fully mixed cells, all connected in series. The plug flow cell was designed to represent the processes of advection and dispersion, while the fully mixed cells simulate the kinetic reactions of phosphorus within the river system. To account for the natural transformation and decay of phosphorus as it moves through the water, a first-order kinetic reaction was integrated into the model.

To solve the model and predict phosphorus behavior, Laplace transformation was employed. This mathematical approach allowed the derivation of analytical solutions that describe the phosphorus dynamics in terms of advection, dispersion, and nutrient kinetics. These analytical solutions were then implemented in user-friendly software and developed using the C-Sharp programming language. The software was capable of forecasting both temporal and spatial fluctuations in phosphorus concentrations within the river, serving as a valuable tool for the ongoing monitoring and management of surface water quality.

Fig. 7 The description of the sampling points within Afe Babalola University Ado Ekiti (ABUAD)

The accuracy of the HCIS model was validated through a two-pronged approach. Hypothetical data were first used to test the model's predictive capabilities under controlled scenarios, followed by validation with real-world field data. The field data were collected from eight strategic sampling locations along River Ureje over several months, concluding on 11th September 2023 to 4th March 2024. The model's predictions were compared with the observed phosphorus concentrations in the river, and the results confirmed the model's effectiveness in simulating the transport of phosphorus within a natural river system. This validation demonstrated that the HCIS model is a reliable tool for predicting nutrient movement and can be instrumental in water quality management.

3.3. The Hybrid Model Parameters and Setup

The residence period of pollutants in a hybrid unit of the HCIS model T1, T2, and T3 can be calculated. These characteristics, which are dependent on the dispersion coefficient and hybrid unit size, have been tested to satisfy the Peclet number ($P_e = \frac{\Delta x u}{D_L} \geq 4$). According to the sampling points depicted in Figure 7, the selected stretch of the Ureje is divided into eight reaches. Each reach will be subdivided into eight hybrid units, each with its own unit size (Δx) and model parameters (see Figure 8).

The initial stage in using this hybrid model to assess the amount of nutrients in the river is to estimate the size of each unit (Δx), which is affected by the longitudinal dispersion coefficient (DL), mean flow velocity, and peclet number (Pe). As a result, Δx will be chosen in such a way that (Pe =Δx u / D_L) must be equal to or greater than 4. (Ghosh et al., 2004; Kumarasamy et al., 2011). By dividing the length of each reach (RL) by the projected hybrid unit size(x), the number of hybrids required between two of the selected spots on the reach will be calculated:

$$n = \frac{RL}{\Delta x} \tag{14}$$

The empirical approach established by Etemad-Shahidi and Taghipour (2012) to determine the DL is shown in Eqs. 15 – 16 below. The fluid properties, channel geometrics, and hydraulic features of the reaches all influence these equations. They're also crucial characteristics for estimating the distribution of solute concentration in a body of water.

If W/ H ≤ 30.6,

$$D_L = 15.49 \left(\frac{W}{H}\right)^{0.78} \left(\frac{u}{U_*}\right)^{0.11} * HU_* \tag{15}$$

Else if greater,

$$D_L = 14.12 \left(\frac{W}{H}\right)^{0.61} \left(\frac{u}{U_*}\right)^{0.85} * HU_* \tag{16}$$

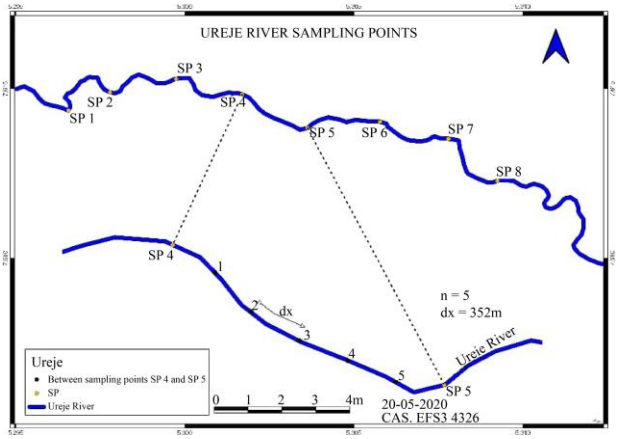

Fig. 8 Schematic diagram of Ureje River illustrating the number of Hybrid units between the study area reaches the size of hybrid units ((Δx) between sampling points taking from SP4 to SP5

Table 1. Model parameters and flow characteristics of ureje river during the research period

	REACHES						
River properties/ HCIS model parameters	**SP1 – SP2**	**SP2 – SP3**	**SP3 – SP4**	**SP4 – SP5**	**SP5 – SP6**	**SP6 – SP7**	**SP7-SP8**
L(m)	2800	1750	2540	1550	2200	1650	1850
Pe	5	5	5	5	5	5	5
u(m/s)	0.45	0.55	0.5	0.43	0.6	0.4	0.45
D_L (m^2/s)	25.38	25.86	27.48	30.26	22.69	22.25	25.34
Δx (m)	282	235	276	352	189	278	280
T_1 (s)	125.33	190.96	202.92	223.48	167.58	164.28	125.33
T_2 (s)	234.43	238.7	253.65	279.36	209.48	205.35	234.43
T_3 (s)	515.11	525.15	558.03	614.59	460.87	451.78	515.11
Number of hybrid units	10	8	10	5	12	6	7

The Ureje River provided the phosphorus data for this study. The first sample point was used to assess flow characteristics, average channel geometry, and the dispersion coefficient for the initial river reach. After calculating the values of DL and Δx, the model parameters T1, T2, and T3 were estimated using Equations (15) to (17). Table 2 presents the Peclet number (Pe), longitudinal dispersion coefficient (DL), hybrid unit size (Δx), model parameters (T1, T2, T3), and the total number of hybrid units used. These parameters were then applied in the HCIS model to estimate the results.

4. Results And Discussion

4.1. Testing of Phosphorus Transport with Synthetic Data

The suggested model was initially validated using synthetic data to investigate the HCIS-P model's responses for a specific data set. The empirical equations for a given value of u and DL that fulfills the Peclet number Pe 4 were used to calculate the model parameters (T1, T2, and T3) (Gosh,2001). The impacts of phosphorus uptake by algae and the respiration rate of algae, as well as the precipitation of phosphorus to inorganic sediment, were considered when simulating the Phosphorus pollutant in the river at various places along the flow direction using the established model. In addition, the model showed the effect of the rate of phosphorus release from the sediment. Some kinetic and chemical characteristics were estimated from the literature by Brown and Barnwell (1987), and their values are given in Table 3.

Real but random river geometry is used to generate data sets. Using equations, the data is used to calibrate the size of each hybrid unit and estimate the resident duration T1, T2, and T3 in each hybrid cell (3.1 - 3.3). The phosphorus concentration value for the point source influent (CR) is set to 1.0 mg/l. The HCIS-P model was used to simulate phosphorus concentration using synthetic data before modeling observed and simulated ammonia concentration for the Ureje River. Two distinct orthophosphate precipitation rate coefficients (0.001 and 0.005 per minute) were employed in this study to examine the effectiveness of the proposed model on phosphorus concentration simulation while keeping the other model parameters constant. The findings of each hybrid unit at varied orthophosphate concentrations at the end In order to understand the influence of the parameter on phosphorus concentration using the new model, the precipitation rate coefficients are compared. T1, T2, and T3 are the residence time parameters necessary to execute the HCIS- P model. T1= 1.7min, T2 = 2.3min, and T3 = 6.0min are the model parameters utilized, which were taken from Ghosh et al. (2008). The size of each hybrid unit was decided to be Δx = 200m, and the Peclet number was chosen to be 6, which meets the Peclet number criterion Pe ≥ 4 (Kumarasamy, 2007). The reach is 1600 meters long and is made up of eight hybrid units. The model's performance takes into account parameters such as residence time, orthophosphate precipitation rate coefficient, algal growth and respiration rate, algal biomass supply, and rate of phosphorus release from the algae in the sediment and initial phosphorus concentration. Simulated unit step and impulse responses at the conclusion of each hybrid unit are plotted and examined at orthophosphate precipitation rate coefficients of 0.001 and 0.005 per minute. The phosphorus concentration vs time curve depicts the behavior of phosphorus concentration as time passes. The pace at which phosphorus decays is determined by the orthophosphate precipitation rate coefficient and the concentration of phosphorus is therefore simulated along a series of hybrid units.

Figure 9 shows the computed response of the unit step function at the end of the first hybrid unit. The outcome of phosphorus concentration over time for different values of orthophosphate precipitation rate coefficient α_p (0.001 and 0.005 per min), with all other parameters held constant, is shown in the picture. It's possible the rate of transmission of phosphorus pollutants in the water body as it flows downstream is affected by variations in the orthophosphate precipitation rate coefficient (αp). The sewage from the lower value of α_p also reaches the boundary concentration faster than the effluent from the larger value of α_p. For the same set of parameters and α_p values, Figure 11 displays the response of the unit impulse function at the conclusion of the first hybrid unit. The peak concentration decreases as the orthophosphate precipitation rate coefficient (αp) in the river increases, as seen in the graph. When (αp) = 0.005 per minute was compared to the peak concentration, there was a 2.73 percent drop to when αp = 0.001 per min.

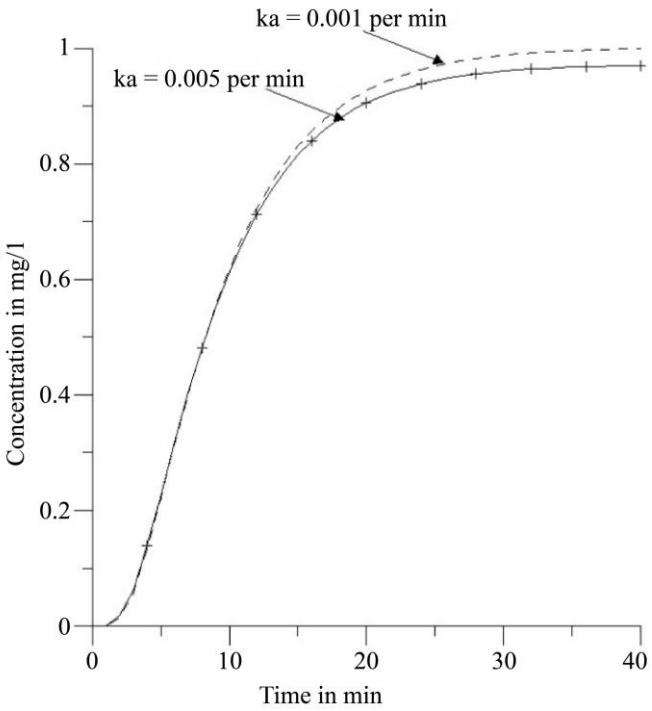

Fig. 2 Unit step responses of the HCIS–P model, with decay rate coefficient, ka = 0.001 per min and 0.005 per min at the end of first hybrid units for T_1 = 1.7 min, T_2 = 2.3 min, T_3= 6.0min, u = 20 m/min and Δx = m

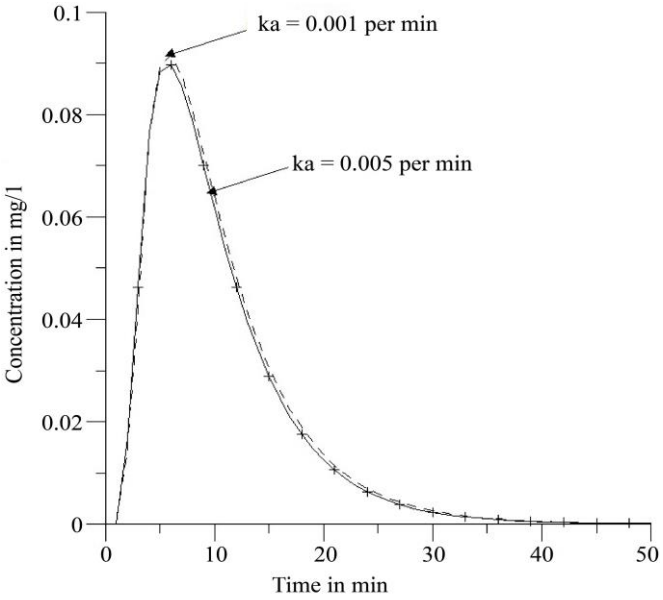

Fig. 10 Unit impulse responses of the HCIS–P model, with decay rate coefficient, Ka = 0.001 per min and 0.005 per min at the end of first hybrid units for T_1 = 1.7 min, T_2 = 2.3 min, T_3= 6.0min, u = 20 m/min and Δx = 200 m

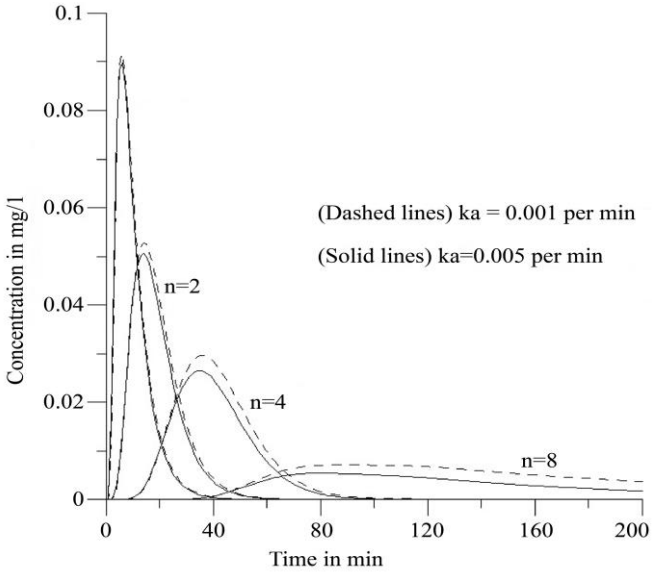

Fig. 11 Unit impulse responses of the HCIS–P model, with decay rate coefficient, α_p = 0.001 per min and 0.005 per min, at the end of first at the end of first (n = 1), second (n = 2), fourth (n = 4) and eighth (n = 8) hybrid units T_1 = 1.7 min, T_2 = 2.3 min, T_3= 6.0min, u = 20 m/min and Δx = 200 m

The generated model is used to simulate the unit impulse responses of the HCIS-P model at the conclusion of the first, second, fourth, and eighth hybrid units for different orthophosphate precipitation rate coefficients (Ka) (0.001 and 0.005 per min). As the number of hybrid units rose, the peak concentration and time to peak both decreased. Furthermore, as the phosphorus pollutant flowed downstream in the river system, its concentration was reduced. With an increase in the number of hybrid units, the C-t distribution revealed a longer tail in the falling limb. The suggested hybrid model can forecast the peak concentration value and time to peak with satisfactory accuracy. The C-t profile was getting close to a fast rate of spread out of the phosphorus concentration in the river, causing a bell-shaped distribution as it traveled downstream.

4.2. Testing of the HCIS-P Model Using Field Data

From September 2023 to March 2024, the observed Phosphorus concentration values from several sample stations along the Ureje River were utilized to simulate the HCIS-P model, with the simulation results serving as a comparison. To run the model simulation, the observed data from phosphorus concentration in mg/l from Sampling Point One (SP1) at bi-weekly intervals from September 11th, 2023, to March 4th, 2024, were used as step input data to run the Hybrid Cell in Series Model (HCIS-P) in order to generate simulated phosphorus concentrations at other sampling points such as SP2 to SP8 at the downstream location, as shown in Table 3. The resultant simulated data is then compared to the initial observed data obtained from Sampling Points 2 to 8, as indicated in Figures 12 to 18. The HCIS-P model was calibrated for simulated phosphorus concentrations in steady-state conditions. The calibration was carried out using real flow data from September 2023 to March 2024 at sampling locations SP1 to SP8 (Table 4) and the upstream values of observed phosphorus concentration as the boundary condition. Calibration was done using a procedure in which one or two parameters were modified at a time while the other parameters remained constant.

The implications of new parameter values on the simulated outcomes were investigated using a computer simulation. Calibration was accomplished by tweaking model parameter values until a satisfactory simulation was obtained. As a result, the model's calibration was intended to modify the kinetics parameters to optimal simulation conditions until the predicted values and measured concentration data were agreed upon. Both the observed and simulated values of phosphorus concentration at the various sampling points, such as SP 2, 3, 4, 5, 6, 7, and 8, were similarly matched in pattern and occurrence during the period between 11th September 2023 and 4th March 2024, as shown in Figures 14 to 20. The dates are September 11th, 2023, through March 4th, 2024. With a rise in flow conditions, the detected phosphorus concentration in the stream increased, generating a surge in pollutant conveyance downstream. The rise in flow was caused by an increase in discharge into the river as a result of the heavy rain. Similarly, from the 5th of November to the 17th of December 2023, there was a drop in phosphorus, and both measured and simulated data revealed a concentration. A low flow rate caused the phosphorus concentration to drop during these times. The trends in phosphorus concentration were also compared during the months of January to March 2024, and it was discovered that the measured and observed values agreed.

Table 2. Summary Table of the measured phosphorus concentration at sampling points 1 to 8 to include the average discharge (M/s^{-3}

Date	SP1 Observed	SP2 Observed	SP3 Observed	SP4 Observed	SP5 Observed	SP6 Observed	SP7 Observed	SP8 Observed	Flow
11/9/2023	0.220	0.210	0.220	0.200	0.210	0.190	0.195	0.180	1.550
25/9/2023	0.260	0.255	0.262	0.255	0.262	0.260	0.258	0.263	1.600
9/10/2023	0.280	0.275	0.280	0.260	0.240	0.235	0.240	0.230	1.400
23/10/2023	0.290	0.280	0.285	0.260	0.265	0.250	0.260	0.255	1.350
6/11/2023	0.090	0.095	0.080	0.090	0.070	0.080	0.083	0.078	0.150
20/11/2023	0.085	0.082	0.081	0.079	0.079	0.081	0.080	0.078	0.130
4/12/2023	0.057	0.053	0.050	0.056	0.058	0.053	0.052	0.055	0.090
18/12/2023	0.055	0.054	0.042	0.045	0.049	0.049	0.048	0.048	0.093
1/1/2024	0.090	0.080	0.085	0.070	0.075	0.080	0.065	0.066	0.700
15/1/2040	0.050	0.053	0.070	0.057	0.058	0.052	0.057	0.051	0.056
29/1/2024	0.080	0.065	0.067	0.066	0.056	0.050	0.052	0.051	0.680
5/2/2024	0.100	0.090	0.095	0.100	0.089	0.096	0.095	0.092	0.160
19/2/2024	0.116	0.097	0.096	0.094	0.094	0.094	0.093	0.092	1.200
4/3/2024	0.095	0.095	0.090	0.092	0.090	0.092	0.089	0.090	1.150

Table 3. Summary table of phosphorus concentration generated in sampling points 2 to 8 when values from SP1 were inputed into the HCIS-P model

Date	SP1 Simulated	SP Simulated	SP3 Simulated	SP4 Simulated	SP5 Simulated	SP 6 Simulated	SP7 Simulated	SP8 Simulated
11/9/2023	0.220	0.208	0.250	0.150	0.140	0.130	0.160	0.150
25/9/2023	0.260	0.240	0.270	0.220	0.210	0.220	0.254	0.240
9/10/2023	0.280	0.260	0.240	0.290	0.237	0.230	0.236	0.245
23/10/2023	0.290	0.250	0.282	0.259	0.240	0.245	0.256	0.241
6/11/2023	0.090	0.150	0.044	0.089	0.067	0.075	0.090	0.072
20/11/2023	0.085	0.060	0.068	0.095	0.094	0.095	0.100	0.072
4/12/2023	0.057	0.051	0.047	0.070	0.055	0.048	0.070	0.075
18/12/2023	0.055	0.052	0.070	0.044	0.040	0.044	0.044	0.040
1/1/2024	0.090	0.076	0.130	0.069	0.066	0.075	0.059	0.085
15/1/2040	0.050	0.049	0.065	0.040	0.060	0.070	0.070	0.080
29/1/2024	0.080	0.085	0.062	0.059	0.051	0.044	0.080	0.043
5/2/2024	0.100	0.095	0.090	0.140	0.120	0.110	0.089	0.078
19/2/2024	0.116	0.150	0.122	0.091	0.070	0.050	0.075	0.120
4/3/2024	0.095	0.075	0.085	0.060	0.085	0.079	0.083	0.082

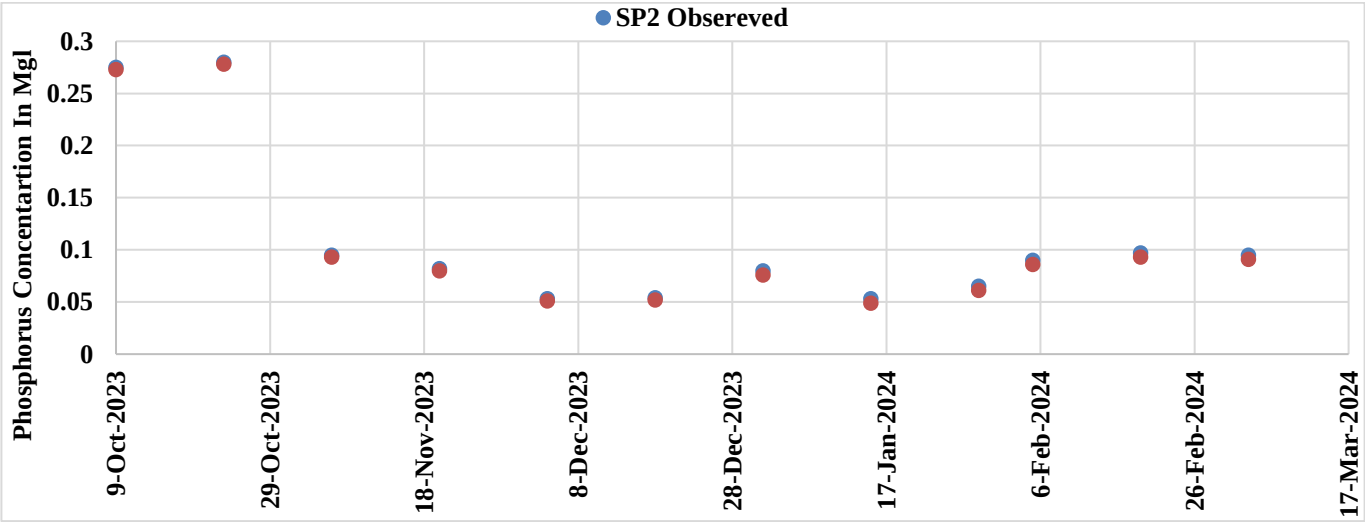

Fig. 32 Measured and Simulated phosphorus concentration at SP2

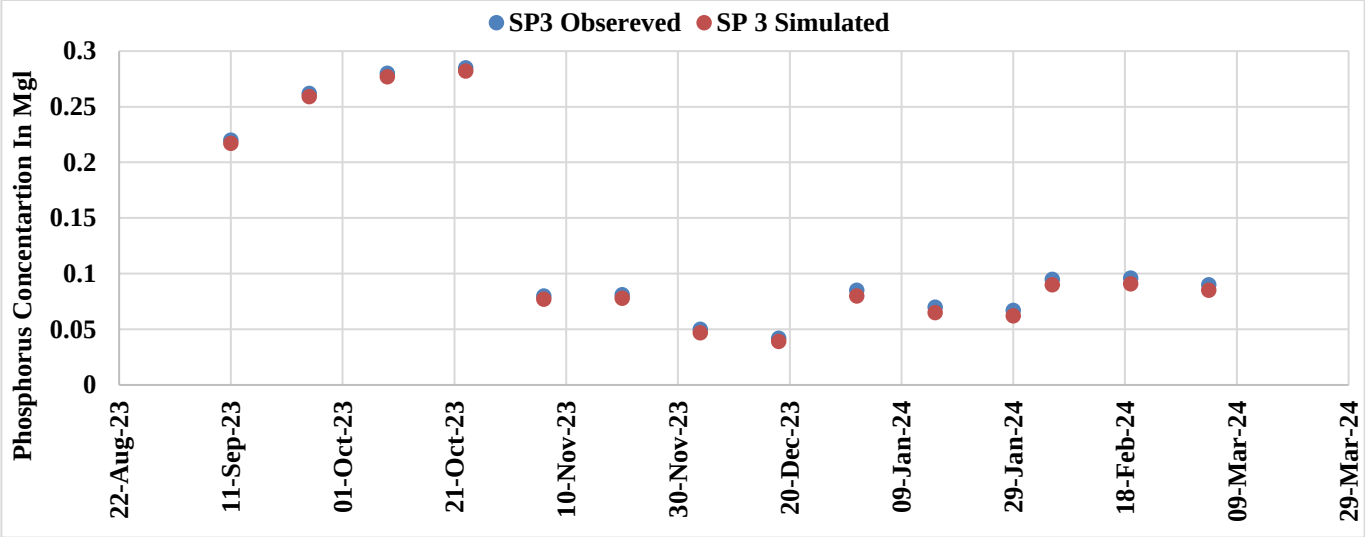

Fig. 13 Measured and Simulated phosphorus concentration at SP3

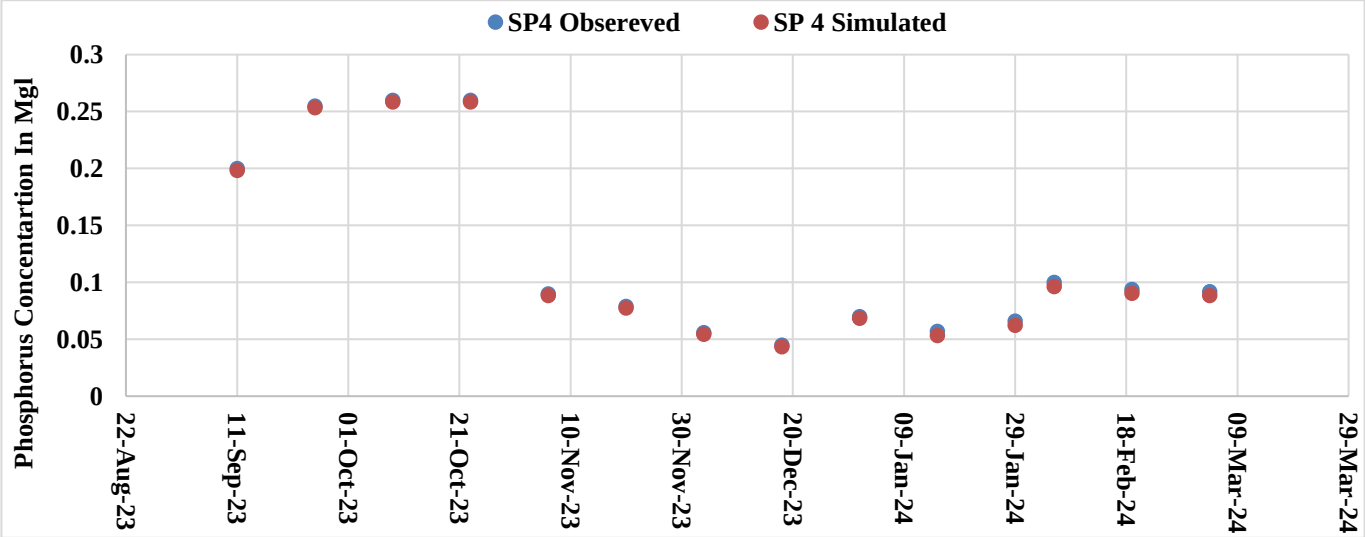

Fig. 14 Measured and Simulated phosphorus concentration at SP4

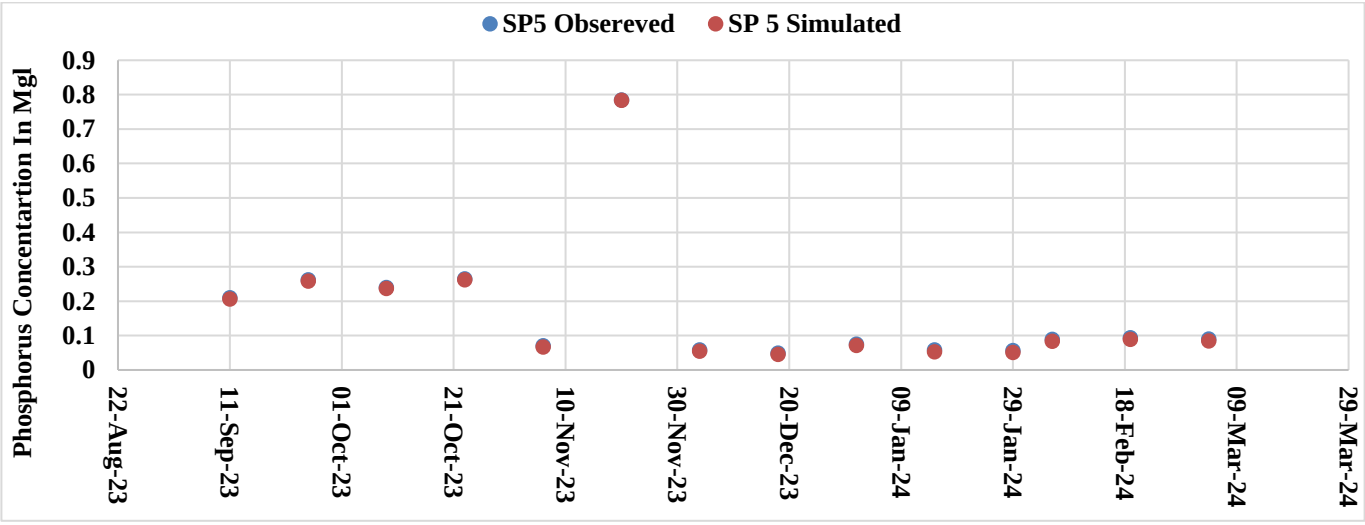

Fig. 15 Measured and Simulated phosphorus concentration at SP5

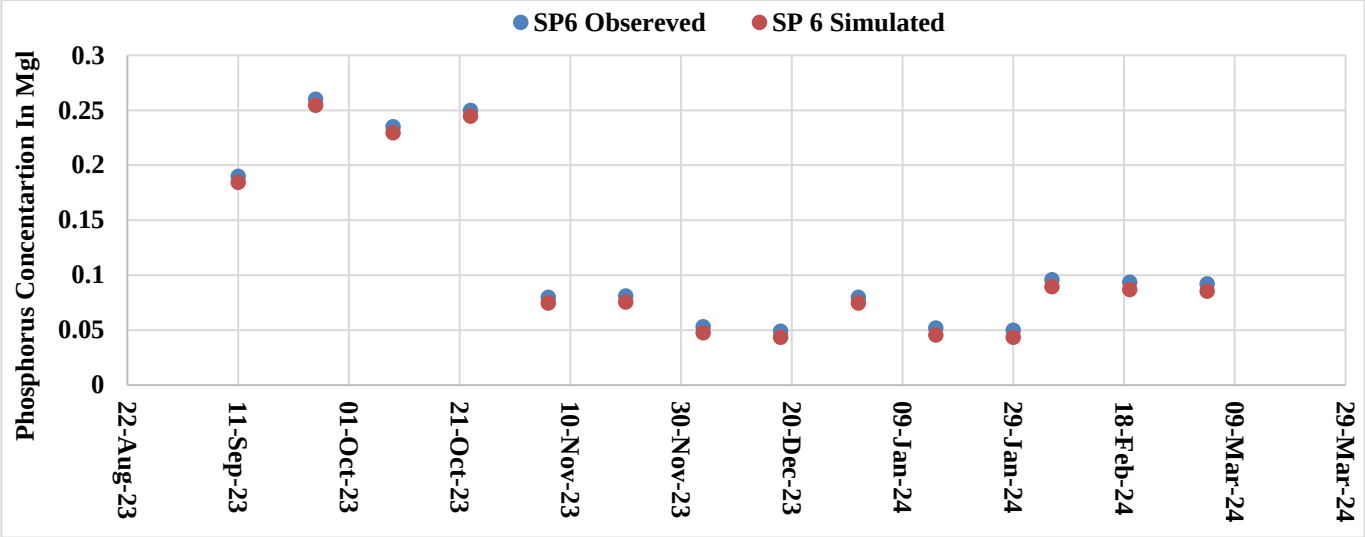

Fig. 16 Measured and Simulated phosphorus concentration at SP6

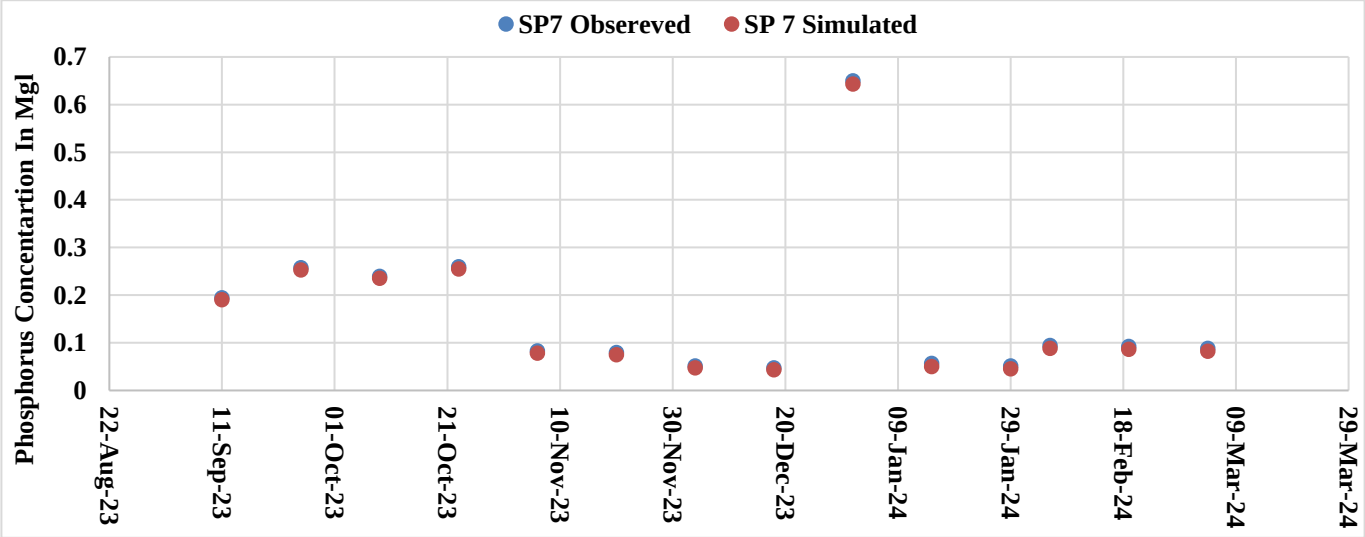

Fig. 17 Measured and Simulated phosphorus concentration at SP7

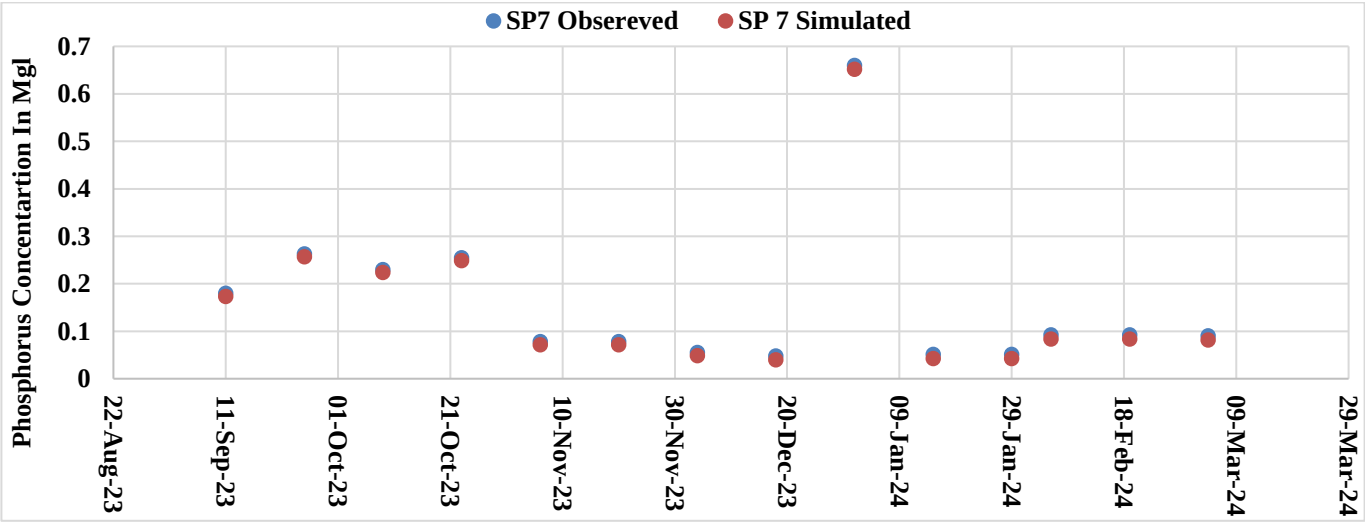

Fig. 18 Measured and Simulated phosphorus concentration at SP5

5. Conclusion

In conclusion, the Hybrid Cell in Series (HCIS) Model has demonstrated its effectiveness as a reliable alternative for solving solute transport in surface water bodies. Its strength lies in its ability to simulate both advection and dispersion processes by combining a plug flow cell with two well-mixed cells in series. This configuration provides the model with an advantage over other water quality monitoring tools, particularly in its capacity to simulate nutrient movement with greater precision. One of its distinguishing features is the plug flow component, which enables the model to accurately predict the first-time arrival of solutes at various sampling points—a critical aspect that many traditional models fail to capture effectively.

The effectiveness of the HCIS model was validated through phosphorus concentration simulations in the Ureje River, using real-world data collected from multiple sampling stations over several months. In the simulation, key hydrodynamic parameters such as flow characteristics, channel geometry, and dispersion coefficients were integrated to create a realistic representation of the river system. Additionally, the model factored in nitrification, denitrification, and algal growth rates during nutrient simulations, allowing for a comprehensive analysis of nutrient transport and transformations.

The model's predictions of nutrient concentration changes closely matched the actual measured values, demonstrating its robustness even under varying conditions of precipitation and flow rates. Given these capabilities, the HCIS model emerges as a valuable tool for river quality monitoring agencies, providing them with accurate assessments of nutrient pollution levels. This is particularly important for managing and mitigating the impacts of nutrient overloading in water bodies, which can lead to problems like eutrophication. However, it is also important to acknowledge certain limitations of the model. For instance, it assumes that river reaches are prismatic (uniform in cross-section), and it applies constant parameters within each reach, which may not fully reflect the complexities of natural river systems. Despite these constraints, the HCIS model shows great potential for advancing nutrient transport predictions and can significantly enhance water quality management efforts in surface water systems. Lastly, several strategies can be employed to mitigate phosphorus pollution in rivers like the Ureje. One key approach is the implementation of buffer zones along riverbanks, where vegetation absorbs and filters out excess phosphorus from agricultural runoff before it reaches the water. Additionally, promoting sustainable agricultural practices, such as reducing fertilizer use and optimizing nutrient management, can minimize phosphorus runoff. Constructed wetlands can also be introduced.

References

[1] Olowe Kayode Oluwafemi, Oyebode Oluwadare, and Dada Temidire, "Water Quality Assessment of River Elemi and Ureje in Ado Ekiti, Nigeria," *Civil & Environmental Engineering*, vol. 24, no. 6, pp. 1-5, 2017. [CrossRef] [Google Scholar] [Publisher Link]

[2] O.O. Ayeni et al., "Physico-Chemical and Bacteriological Assessments of Shallow Well Water Samples during the Dry and Rainy Seasons," *Nigerian Journal of Technological Development*, vol. 20, no. 2, pp. 43-52, 2023. [CrossRef] [Google Scholar] [Publisher Link]

[3] M Kumarasamy, "Modeling Ammonia-Nitrogen Fate and Transport in UMgeni River," *Science without Borders (WISWB)–Indaba*, 2017. [Google Scholar]

[4] Chengjian Liu et al., "Time-Lag Effect: River Algal Blooms on Multiple Driving Factors," *Frontiers in Earth Science*, vol. 9, pp. 1-12, 2021. [CrossRef] [Google Scholar] [Publisher Link]

[5] M.V. Kumarasamy, "Deoxygenation and Reaeration Coupled Hybrid Mixing Cells Based Pollutant Transport Model to Assess Water Quality Status of a River," *International Journal of Environmental Research*, vol. 9, no. 1, pp. 341-350, 2015. [CrossRef] [Google Scholar] [Publisher Link]

[6] Muthukrishnavellaisamy Kumarasamy et al., "Semianalytical Solution for Nonequilibrium Sorption of Pollutant Transport in Streams," *Journal of Environmental Engineering*, vol. 137, no. 11, pp. 1066-1074, 2011. [CrossRef] [Google Scholar] [Publisher Link]

[7] M. Yuceer, and M.A. Coskun, "Modeling Water Quality in Rivers: A Case Study of Beylerderesi River in Turkey," *Applied Ecology and Environmental Research*, vol. 14, no. 1, pp. 383–395, 2016. [CrossRef] [Google Scholar] [Publisher Link]

[8] Kayode O. Olowe, and Muthukrishna Vellaisamy Kumarasamy, "Assessment of Some Existing Water Quality Models," *Nature Environment & Pollution Technology*, vol. 17, no. 3, pp. 939-948, 2018. [CrossRef] [Google Scholar] [Publisher Link]

[9] Muthukrishnavellaisamy Kumarasamy et al., "Hybrid Model Development for the Decaying Pollutant Transport in Streams," *International Journal of Environment and Waste Management*, vol. 12, no. 2, pp. 1-16, 2013. [CrossRef] [Google Scholar] [Publisher Link]

[10] XU Wei-Gang et al., "Effects of Vegetation on River Flow: A Review," *Chinese Journal of Applied Ecology*, vol. 24, no. 1, pp. 251–259, 2013. [Google Scholar] [Publisher Link]

[11] Donald M. Anderson, Patricia M. Glibert, and Joann M. Burkholder, "Harmful Algal Blooms and Eutrophication: Nutrient Sources, Composition, and Consequences," *Estuaries*, vol. 25, no. 4, pp. 704-726, 2002. [CrossRef] [Google Scholar] [Publisher Link]

[12] Jaeyoung Kim, John R. Jones, and Dongil Seo, "Factors Affecting Harmful Algal Bloom Occurrence in a River with Regulated Hydrology," *Journal of Hydrology: Regional Studies*, vol. 33, pp. 1-14, 2021. [CrossRef] [Google Scholar] [Publisher Link]

[13] Narayan C. Ghosh, Govinda C. Mishra, and Muthukrishnavellaisamy Kumarasamy, "Hybrid-Cells-in-Series Model for Solute Transport in Streams and Relation of Its Parameters with Bulk Flow Characteristics," *Journal of Hydraulic Engineering*, vol. 134, no. 4, pp. 497-502, 2008. [CrossRef] [Google Scholar] [Publisher Link]

[14] Prakash R. Kannel et al., "A Review of Public Domain Water Quality Models for Simulating Dissolved Oxygen in Rivers and Streams," Environmental Modeling & Assessment, vol. 16, no. 2, pp. 183–204, 2011. [CrossRef] [Google Scholar] [Publisher Link]